

Using Photoelectron Spectroscopy and Quantum Mechanics to Determine d-Band Energies of Metals for Catalytic Applications

Timo Hofmann,^{†,*} Ted H. Yu,[‡] Michael Folse,[†] Lothar Weinhardt,^{†,§,⊥,¶} Marcus Bär,^{†,#,∇} Yufeng Zhang,^{†,○} Boris V. Merinov,[‡] Deborah J. Myers,[◆] William A. Goddard, III,[‡] and Clemens Heske^{†,⊥,¶,■,*}

[†]Department of Chemistry, University of Nevada, Las Vegas (UNLV), 4505 S. Maryland Parkway, Las Vegas, Nevada 89154-4003, United States

[‡]Materials and Process Simulation Center, m/c 139-74, California Institute of Technology, 1200 East California Boulevard, Pasadena, California 91125, United States

[§]Experimentelle Physik VII, Universität Würzburg, Am Hubland, D-97074 Würzburg, Germany

[⊥]Institute for Photon Science and Synchrotron Radiation and [¶]ANKA Synchrotron Radiation Facility, Karlsruhe Institute of Technology (KIT), Hermann-v.-Helmholtz-Platz 1, 76344 Eggenstein-Leopoldshafen, Germany

[#]Solar Energy Research, Helmholtz-Zentrum Berlin für Materialien und Energie GmbH, Hahn-Meitner-Platz 1, D-14109 Berlin, Germany

[∇]Institut für Physik und Chemie, Brandenburgische Technische Universität Cottbus, Konrad-Wachsmann-Allee 1, D-03046 Cottbus, Germany

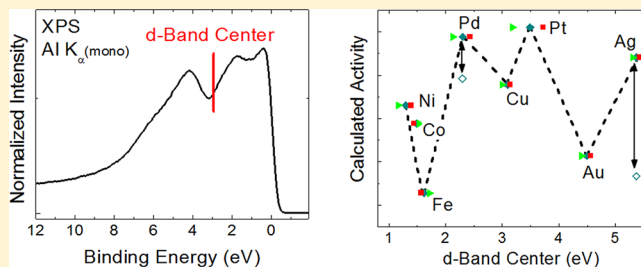
[○]Department of Physics, Xiamen University, 422 Si-Ming-Nan-Lu, Xiamen, Fujian, 361005, People's Republic of China

[◆]Chemical Sciences and Engineering Division, Argonne National Laboratory, 9700 S. Cass Avenue, Argonne, Illinois 60439, United States

[■]Institute for Chemical Technology and Polymer Chemistry, Karlsruhe Institute of Technology (KIT), Engesserstrasse 18/20, 76128 Karlsruhe, Germany

Supporting Information

ABSTRACT: The valence band structures (VBS) of eight transition metals (Fe, Co, Ni, Cu, Pd, Ag, Pt, Au) were investigated by photoelectron spectroscopy (PES) using He I, He II, and monochromatized Al K α excitation. The influence of final states, photoionization cross-section, and adsorption of residual gas molecules in an ultrahigh vacuum environment are discussed in terms of their impact on the VBS. We find that VBSs recorded with monochromatized Al K α radiation are most closely comparable to the ground state density of states (DOS) derived from quantum mechanics calculations. We use the Al K α -excited PES measurements to correct the energy scale of the calculated ground-state DOS to approximate the “true” ground-state d-band structure. Finally, we use this data to test the d-band center model commonly used to predict the electronic-property/catalytic-activity relationship of metals. We find that a simple continuous dependence of activity on d-band center position is not supported by our results (both experimentally and computationally).



1. INTRODUCTION

Many industrial catalysts for the production of valuable chemicals and extraction of energy from fuels involve transition metals.^{1–3} These catalysts have mostly been developed empirically, that is, without guidance from the detailed electronic structures likely to play an important role in the selectivity and activity. A promising tool to provide such detailed electronic structural information is photoelectron spectroscopy (PES), which has been widely used to provide experimental information of the electronic structure of transition metals.^{4–6} A particularly important application is

for polymer electrolyte membrane fuel cells (PEMFCs), in which platinum (Pt)-containing catalysts are often employed to catalyze the oxygen reduction reaction (ORR). The high costs^{7,8} of PEMFC are mainly associated with the expense of the Pt-containing catalysts,⁹ currently required to obtain satisfactory performance. Indeed, the limited efficiency and lifetimes⁷ of these catalysts are currently the main barriers to

Received: April 5, 2012

Revised: October 23, 2012

Published: October 25, 2012

commercialization. This has triggered vast research efforts to find a catalytic material that combines high catalytic activity with low cost and high stability. A multitude of pathways to improve current catalysts and to explore novel catalytic materials has been pursued, ranging from the reduction of the utilized amount of Pt^{10–12} to the synthesis of non-noble catalysts¹³ and nanocatalysts of particular shape¹⁴ and/or with a deliberate mixture of nonplatinum metal constituents.^{15–17} These developments have often been guided by theoretical calculations to predict the catalytic activity of a particular surface.^{18–25} Most notably, Hammer and Nørskov developed the “d-band center model” that correlates the electronic structure of a (transition) metal, through calculation of the weighted mean energy of its d-band (“d-band center”), to its reactivity.^{18,22,23,26} Indeed, this model is in excellent agreement with some experimental results,^{27–29} while some authors find significant differences.^{25,30,31} The criticism typically relates to the poor correlation between the d-band center and reactivity measures (or changes in the reactivity measures) inconsistent with the model predictions, while the published d-band center values are often uncontested. Centroid values reported in the literature, however, often suffer from poor correlation between experimental and theoretical²⁹ values. Furthermore, the proper definition, experimental determination, and analysis of the d-band center is unclear and varies throughout literature, both for computational³² and experimental results.

It is hence the purpose of the present paper (1) to perform a careful and detailed analysis of photoelectron spectra recorded with various lab-based excitation sources for a range of metals relevant to catalysis, (2) to compare these with theoretical ground state density-of-states (DOS) calculations, (3) to combine the experimental data and DOS calculations to derive the “true” valence band structures (VBS) and thus to refine their d-band center energies, (4) to provide a detailed discussion on the methodology of measurement and analysis of d-band centers and compare them to values reported in the literature and, finally, (5) to compare these d-band centers to published catalytic activities, thereby providing an experiment-based analysis of the validity of the “d-band center model”.

In section 2 we outline various details of the experimental and theoretical methodologies. The results are analyzed and discussed in section 3, and d-band centers for all eight metals are determined and compared to published catalytic activities. Finally, conclusions are presented in section 4.

2. EXPERIMENTAL AND THEORETICAL METHODS

2.1. Experimental Methods. Polycrystalline metal foils (purity of 99.9% or higher) were cleaned by Ar⁺ ion sputtering using ion energies between 0.5 and 5 keV. Surface cleanliness was verified by recording Mg and Al K α -excited PES detail spectra of the C 1s and O 1s energy region. Sputtering was continued until no or only trace amounts of carbon and oxygen could be detected on the sample surface. Valence band PES measurements were performed using He I ($h\nu = 21.22$ eV) and He II ($h\nu = 40.82$ eV) ultraviolet excitation lines (ultraviolet photoelectron spectroscopy, “UPS”) and monochromatized Al K α ($h\nu = 1486.58$ eV) X-ray radiation (X-ray photoelectron spectroscopy, “XPS”). The UPS spectra were excited with a Vacuum Generators (VG) He discharge source and recorded with a SPECS PHOIBOS 150 MCD electron analyzer. For UPS, a negative bias voltage of 12 or 15 V was applied to the sample to accelerate electrons of low kinetic energy and therefore to allow for an accurate determination of the

secondary electron cutoff. The XPS spectra were excited with a Scienta MX650 X-ray source (consisting of an SAX-100 X-ray source and an XM-780 X-ray monochromator) and recorded with a Scienta R4000 electron analyzer. The energy scale of the two electron spectrometers was calibrated using the kinetic energy positions of the most prominent photoemission lines of copper, silver, and gold.³³ The experiments were performed in two connected ultrahigh vacuum (UHV) systems at base pressures of 5×10^{-10} mbar or better.

2.2. Computational Methods. Periodic quantum mechanics (QM) calculations were carried out with the SeqQuest code,^{34,35} which employs Gaussian basis functions at the optimized double- ζ plus polarization level rather than the plane-wave basis often used in periodic systems. We used the Perdew–Becke–Ernzerhof (PBE) flavor³⁶ of density functional theory (DFT) in the generalized gradient approximation (GGA)^{37,38} and allowed the up-spin orbitals to be optimized independently of the down-spin orbitals (spin-unrestricted DFT). All calculations were performed with spin optimization. We used small core pseudopotentials with angular momentum projections.^{39,40}

The d-band structures were analyzed with the SeqQuest Post-Analysis Code³⁵ and further broken down into d_{eg} ($d_{x^2-y^2}$, d_{z^2}) and d_{2g} (d_{xy} , d_{yz} , d_{xz}) orbitals. The DOS was broadened by convolution with a 0.5 eV fwhm Gaussian function to approximate the experimental and lifetime broadening of the spectra. Furthermore, the DOS was multiplied with the Fermi function at 300 K to limit the description to occupied electronic states. Additional modifications to the energy axis of the DOS were performed, as described in detail in the Results and Discussion section.

3. RESULTS AND DISCUSSION

3.1. Sample Preparation. XPS survey spectra of pure iron (Fe), cobalt (Co), nickel (Ni), copper (Cu), palladium (Pd), platinum (Pt), silver (Ag), and gold (Au) metal foils, cleaned by Ar⁺ ion sputtering, are shown in Figure 1 (all spectra were normalized to the height of the most prominent peak). Vertical dashed lines indicate the common binding energies for adventitious carbon (284.8 eV)⁴¹ and oxygen (531.0 eV).⁴¹

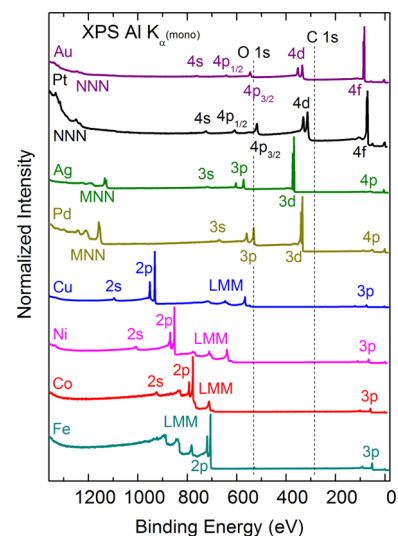


Figure 1. Monochromatized Al K α XPS survey spectra of Ar⁺-sputtered polycrystalline metal samples.

The absence of spectral intensity along these lines shows that the samples were successfully cleaned. XPS spectra of the C 1s and O 1s regions taken after the UPS measurements (not shown here) reveal a small carbon contamination for all metal surfaces (Pt \approx 5–8, Fe \approx 3, Ni \approx 1–2, Co \approx 3–6, Pd \approx 0, Ag \approx 0–1, Au \approx 0–3 atom %). Furthermore, the oxygen-related signals were found to be low on all metals (Pt \approx 0–5, Fe \approx 4, Ni \approx 0–1, Co \approx 2–7, Pd \approx 0, Ag \approx 0–1, Au \approx 0 atom %). The remaining adsorbates are attributed to the adsorption of residual gases at background pressures of 10^{-10} mbar^{42,43} and/or to carbon and oxygen atoms embedded in the surface of the foil. As will be discussed later, such adsorbates can influence the spectral weight distribution of photoemission spectra, in particular when taken in a very surface-sensitive mode (i.e., using UPS).

In addition to monitoring surface cleanliness using XPS core level spectra, UV excitation was employed to determine the secondary electron cutoff and thus the work function of a set of similarly cleaned metal foils. The presence of small amounts of contaminants generally impacts the surface dipole and hence the work function significantly (see, e.g., refs 44 and 45). Table 1 lists the work functions of the metals as determined by UPS

Table 1. Work Functions (WF) of Polycrystalline Metal Foils, as Derived from Secondary Electron Cutoffs of He I-Excited Photoemission Spectra^a

metal	WF (eV)	literature values (eV)
Fe	4.68 \pm 0.10	4.5, ⁴⁹ 4.67 (100), ^{27,49} 4.71 α -phase ¹⁰⁸ 4.81 (111) ^{27,49}
Co	4.92 \pm 0.10	4.89 α -phase, ¹⁰⁸ 5.0 ^{27,49}
Ni	5.21 \pm 0.10	5.04 (110), ²⁷ 5.15, ⁴⁹ 5.22 (100), ²⁷ 5.35 (111) ²⁷
Cu	4.44 \pm 0.10	4.46, ¹⁰⁹ 4.48 (110), ²⁷ 4.53 (112), ²⁷ 4.65, ⁴⁹ 4.94 (111) ²⁷ , 5.10 (100) ²⁷
Pd	5.19 \pm 0.10	5.22, ^{27,49} 5.6 (111) ²⁷
Ag	4.30 \pm 0.10	4.26, ¹² 4.52 (110), ^{27,49} 4.64 (100), ^{27,49} 4.74 (111) ^{27,49}
Pt	5.59 \pm 0.10	5.12 (331), ²⁷ 5.22 (320), ²⁷ 5.27, ¹¹⁰ 5.5, ⁴⁹ 5.64, ²⁷ 5.84 (110), ^{27,49} 5.93 (111) ^{27,49}
Au	5.26 \pm 0.10	5.1, ⁴⁹ 5.31 (111), ^{27,49} 5.37 (110), ^{27,49} 5.47 (100) ^{27,49}

^aLiterature values are listed for single crystals (with surface orientations given in parentheses) and polycrystalline samples.

using He I excitation. We find that the work functions of all metals are well within the range of literature values (third column in Table 1). The good agreement of the work functions with reported values suggests that the here-studied surfaces can serve as “clean” model systems to derive the electronic valence structure.

3.2. Derivation of d-band Centers and the Impact of Photon Energy Variation and Surface Adsorbates. For a proper comparison of the various PES-based approaches to study the electronic structure of transition metals, it is necessary to review the inherent experimental challenges, such that the most meaningful method for evaluation of the d-band structure can be derived. We start by comparing the VBS of the metal foils, as measured by UPS and XPS, in Figure 2. Panels a and b give the valence band spectra taken with He I and He II excitation, respectively, while panel c shows the spectra taken with monochromatized Al K α radiation. Stars mark spectral contributions associated with adsorbed species on the metal surface (as will be discussed below), and short vertical lines give the weighted average energy of the VBS (error bars are in the range of ± 0.05 to ± 0.25 eV and will be given in more detail in conjunction with Table 2 and Figure 5). This energy, which is commonly associated with the d-band center (since s- and p-

contributions to the VBS are relatively small), is derived using the procedure outlined in ref 27. Since this procedure includes integrals over the valence band region, the procedure for defining background boundaries can lead to significant variability in the derived average energy. The contribution of the background that lies within the integration boundaries is shown as a thin line underneath each spectrum; its determination will be discussed in the following.

We start the discussion of proper quantification of the d-band center by addressing the experimental challenges. A closer look at Figure 2 reveals substantially varying spectral weight distributions that reflect the energies and occupation of the valence bands of the different metals and also the significant influence of the excitation energy. For example, all He I-excited spectra (Figure 2a) and some of the He II-excited spectra (Figure 2b) exhibit a strong secondary electron background, which is noticeably reduced for the XPS spectra in Figure 2c. The region of interest, that is, the binding energy range of catalytically active states, is thus superimposed on the slope of the background, leading to challenges to properly separate actual states and background intensity. Furthermore, the spectral weight distributions obtained from He I, He II, and XPS reveal pronounced changes for all samples. This raises the question of which experimentally determined VBS is the best choice to determine the true d-band center for correlation with electrochemical performance. As will be discussed below, we conclude that the use of X-ray excitation spectra is preferable over UV-based approaches.

Photon-energy-dependent changes of the VBS can arise for several reasons. First, variations in the single-electron final state (i.e., free electron state vs band-like character) can have a significant impact—VBSs generally change in width and relative intensity ratios with excitation energy (see, e.g., ref 46 for a study of Cu). In the UPS regime, the VBS is often discussed in terms of final-state effects, which are responsible for the observed line positions and intensities determined by transition-matrix-element modulations,⁴⁷ both because of the angular and radial parts of the transition matrix element.⁴⁸ Also, the nature of the integration over the Brillouin zone (BZ) is important. In UPS, the low photon energies (and thus the low photon momentum) require the availability of suitable final states for transitions that are vertical in momentum space.⁴⁹ In XPS, in contrast, the kinetic energy and thus the momentum (uncertainty) of the photoelectrons is so large that the experiment probes the entire BZ in the final state, since transitions no longer need to be vertical. Furthermore, at these high energies, the significantly larger number of states that are reduced back into the BZ will allow the transition to a final state at essentially any k-value. We further note that all foils studied are of a polycrystalline nature, and thus no predominant crystal orientation is expected. If present, such an orientation could lead to (significant) variations in the VBS, because transitions become dependent on the band structure (in particular the availability of a suitable one-electron final state) along the respective crystal orientation.⁴⁶ Again, this effect is more pronounced for lower photon energies (lower photon momenta). In addition, particular surface orientations have been found to strongly influence the catalytic activity due to changes in the number of available adsorption sites and their geometry (see, e.g., ref 50 for the case of Pt).

Second, cross section effects can also play a significant role in the variation of the VBS. For example, “atomic-type” cross-section effects, where the cross-section varies strongly over a

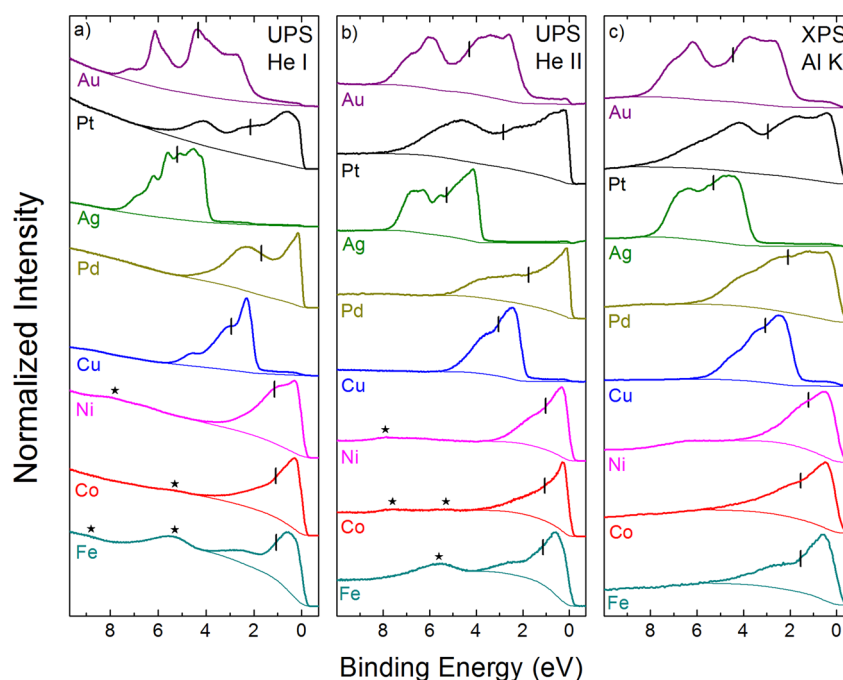


Figure 2. Valence band spectra of different Ar⁺-sputtered polycrystalline metal samples collected using He I (a), He II (b), and monochromatized Al K α (c) excitation. The average energies of the valence band spectral weight (i.e., the d-band center position), derived after subtraction of the background (shown as thin lines underneath each spectrum) and integration, are marked by vertical bars. Adsorbate state contributions are marked with a star (★).

small energy range at low photon energies, are well-known for 4d-group and 5d-group elements (e.g., below 150 eV for Ag^{46,51}).

Third, as already briefly mentioned, the spectral background (slope and curvature) of inelastically scattered electrons also greatly influences the VBS and any numerical integration thereof. The thin lines underneath each spectrum in Figure 2 represent the background determined in the following manner. For spectral features with kinetic energies well above the secondary electron peak, a Shirley background (whose intensity depends on the selected energy range) was subtracted from the measured spectrum.²⁷ For spectra measured with He I, however, the overlap of the spectral features with the secondary electron peaks becomes strong, and hence an additional background subtraction is necessary. In our case, we have subtracted an exponential background prior to the removal of a Shirley background, adding several additional (somewhat arbitrary) parameters in the spectral analysis.

Fourth, variations of the photon energy and hence the kinetic energy of the probed photoelectrons also leads to a variation of the electron inelastic mean free path (IMFP). This, in turn, varies the probed sample volume and the ratio of the sample surface and bulk contributions to the overall spectrum.

For polycrystalline and/or macroscopically disordered samples, it is not likely to find true surface states or even surface resonances—these are generally only found on single-crystalline surfaces with long-range lateral order. In contrast, surface defects might be present and play a role on all surfaces, in particular those of polycrystalline samples (as studied here) and nanoparticles (as most commonly found for real-world catalysts). Hence, the VBS of the here-studied surfaces primarily refers to the bulk states, which exponentially decay into the vacuum at the surface, augmented by contributions from surface defects and, possibly, adsorbates. If surface adsorbates are present (see below), then photoemission

experiments with kinetic energies near the minimum of the IMFP distribution^{52–55} will contain a larger contribution of such spurious surface effects.

It is important to note that both UPS and XPS measure the bulk states that exist throughout the crystal and also dominate the electronic structure at the surface.^{56–58} In other words, the DOS at the surface is made up of contributions originating from the outermost surface layer, as well as deeper-lying layers due to the delocalized nature of electrons in the valence band (for completion, we note that, in contrast, “surface core level shifts” indeed originate from localized core levels at the outermost surface but do not involve delocalized valence states). For the first atomic layer of metals, a narrowing of bulk bands due to the reduced number of neighboring atoms has been reported,^{59,60} while the second layer is often regarded as representative of the bulk.⁶¹ In PES measurements, which effectively consist of an exponentially weighted integration over the probing depth, the first atomic layer accounts for the largest fraction of the overall signal, while the contributions of subsequent atomic layers are (exponentially) attenuated. Hence, VBS measured with PES is most closely related to the surface DOS responsible for the catalytic activity of a material.

Finally, adsorbates such as residual carbon and oxygen species on the surface need to be considered. In comparing the He I and He II UPS spectra with published spectra^{6,42,44,45,62–75} of clean and adsorbate-covered surfaces, adsorbate states can be identified (marked with a star in Figure 2a,b). For example, comparison with literature shows that the main adsorbate contributions in Fe and Co can be ascribed to the oxygen species, and in Ni, Pd, and Pt to carbon monoxide or similar species. On Pt, we further find resonances that can be ascribed to OH groups. For the spectra presented herein, no adsorbate-related peaks were found for Cu, Pd, Ag, Pt, and Au. We find that all adsorbate-induced states are located at binding

Table 2. Metal d-Band Centers (eV)^a

element	He I	He II	Al K α	TDOS	TDOS refined	t _{2g}	e _g	d-sum	theo ^b	expt ^b
Fe	1.06 +0.20/−0.25	1.13 +0.15/−0.20	1.55 +0.10/−0.10	2.14	1.86	1.57	1.71	1.62	0.92 ^{20,22}	
Co	1.08 +0.15/−0.20	1.05 +0.10/−0.10	1.54 +0.10/−0.10	2.54	1.77	1.44	1.53	1.48	1.17, ^{20,22} 2.0 ³²	
Ni	1.14 +0.20/−0.20	1.01 +0.10/−0.10	1.20 +0.05/−0.10	2.35	1.49	1.39	1.16	1.30	1.29, ^{20,22} 1.48, ¹⁸ 1.7 ³²	
Cu	2.93 +0.10/−0.10	3.04 +0.05/−0.05	3.05 +0.05/−0.05	3.02	3.29	3.14	3.00	3.09	2.4, ³² 2.67 ^{18,22}	
Pd	1.68 +0.20/−0.15	1.74 +0.05/−0.10	2.09 +0.05/−0.10	2.44	2.44	2.43	2.13	2.30	1.8, ³² 1.83 ^{20,22}	
Ag	5.19 +0.10/−0.15	5.27 +0.05/−0.05	5.28 +0.05/−0.05	4.31	5.30	5.42	5.30	5.37	4.0, ³² 4.30 ^{20,22}	
Pt	2.14 +0.20/−0.20	2.83 +0.05/−0.05	2.94 +0.05/−0.10	3.37	3.77	3.72	3.18	3.49	2.25, ^{20,22} 2.4, ³² 2.75 ¹⁸	2.356, ⁷⁹ 2.54, ²⁷ 3.45 ⁸¹ 3.98 ²⁹ 4.77 ⁸⁰
Au	4.32 +0.10/−0.15	4.30 +0.05/−0.05	4.45 +0.05/−0.05	4.06	4.62	4.56	4.40	4.49	3.5, ³² 3.56, ^{20,22} 3.91 ¹⁸	4.27 ⁸⁴

^aValues derived from photoelectron spectroscopy (for different excitation energies), theory [total DOS (TDOS), refined TDOS, refined symmetry-resolved (t_{2g} and e_g), and refined summed d-band contributions], and literature [theory (theo) and experiment (expt)]. The “+” and “−” values give the estimated errors in determining the d-band center values. ^bCitations: Ref 18, d-band center of (111) metal surfaces; Ref 22, d-band center of most close-packed surface of each metal; Refs 32, 81, 29, and 84, approximate values taken from Fig. 4 in ref 32, Fig. 8 in ref, Fig. 7 in ref 29, and Fig. 3 in ref 84.

energies larger than the VBS integration window of the metal, that is, the influence of these states on the valence band spectral region (and the d-band center determination) is negligible. However, they are accompanied by a reduction of the DOS close to the Fermi energy^{69,71} and can be interpreted as a charge transfer due to the formation of metal-adsorbate bonds.^{42,67} We expect such a redistribution of spectral weight to shift the center of mass (and hence the derived d-band center values) toward higher binding energy for all UPS spectra in which adsorbate states are found. Nevertheless, since the observed adsorbate intensities are estimated to correspond to submonolayer coverages, we suspect that this shift is generally rather small and that it decreases with increasing excitation energy. In Pd, for example, peaks around 8 and 11 eV can be found after prolonged storage in UHV, which may be derived from the 5 σ - and 1 π -orbitals of adsorbed carbon monoxide,^{42,70,72} and the associated difference in d-band center position was found to be 0.1 eV (see Figure S1 in the Supporting Information). To minimize adsorbate-induced effects, X-ray instead of UV excitation can be used, because the IMFP (and the associated information depth) increases approximately with the square-root of the kinetic energy of the photoelectron.^{52–55}

Taking into account the aspects discussed above, we argue that the determination of the energetic position of d-band centers from XPS spectra appears most favorable, in that it mitigates several experimental (e.g., surface adsorbates) and spectroscopic (e.g., final state effects) complications for a straightforward comparison with such a ground-state property. To analyze this argument more quantitatively, we have determined the d-band center position of the valence band for each metal using He I, He II, and Al K α excitation. Table 2 lists these experimentally determined values, together with our theoretically determined d-band centers, and a comparison with theoretical (“theo”) and experimental positions (“expt”) from the literature. The columns with our theoretical results list the bulk d-band center derived from the total DOS (“TDOS”), the refined TDOS (“TDOS refined”), the partial contributions from the bands with t_{2g} and e_g symmetry, and the sum of these two bands (“d-sum”).

When the experimentally derived d-band center positions with the published theoretical and (where available) experimental values are compared, we find significant differences. There are several possible reasons for the observed differences. First, we note that different calculation approaches can lead to variations in the DOS and/or the associated energy scale.³² Even for a given (fixed) DOS, the calculation of the d-band center value requires the definition of upper and lower integration limits, the choice of which significantly impacts the derived value. To circumvent such complications, some authors have chosen constant (but somewhat arbitrary) limits, for example, 10 eV for occupied states^{27,76} and 15 eV for unoccupied states³² or considered infinite cutoff energies (e.g., refs.19 and 77). In many publications, additional details would be needed to judge the analysis approach, such as integration limits or background shape (e.g., refs.18, 20, 22, 29, 31, and 78–81). As the d-bandwidth significantly varies for the metals under study, we have followed a different approach, namely to vary the upper (high binding energy) integration limit such that only those states are taken into account that are actually resolved by the measurement. For this purpose, we (visually) determined the high energy tail of the d-bands as measured using the three different excitation energies and compared these values with the d-band widths reported for PES studies of clean metals.^{6,42,44,45,62–75} To estimate the variance of this procedure, the d-band center was determined additionally by varying the upper integration limit by ± 0.2 –1.0 eV (depending on excitation energy, direction of variation, position of features, and background shape). The resulting error bars (which are asymmetric) are listed in Table 2 (and will also be shown in Figure 5).

We find that, for a given metal, the such-derived d-band center positions vary up to ≈ 0.5 eV, depending on the excitation energy used. Values determined from the XPS VBS were found to be the highest because the higher-binding-energy states of the VB are more pronounced in this case. Despite significant shape changes in the VB, the differences between the He I- and He II-derived values lie well within the error bars for most metals. The d-band centers of the metals with filled d-

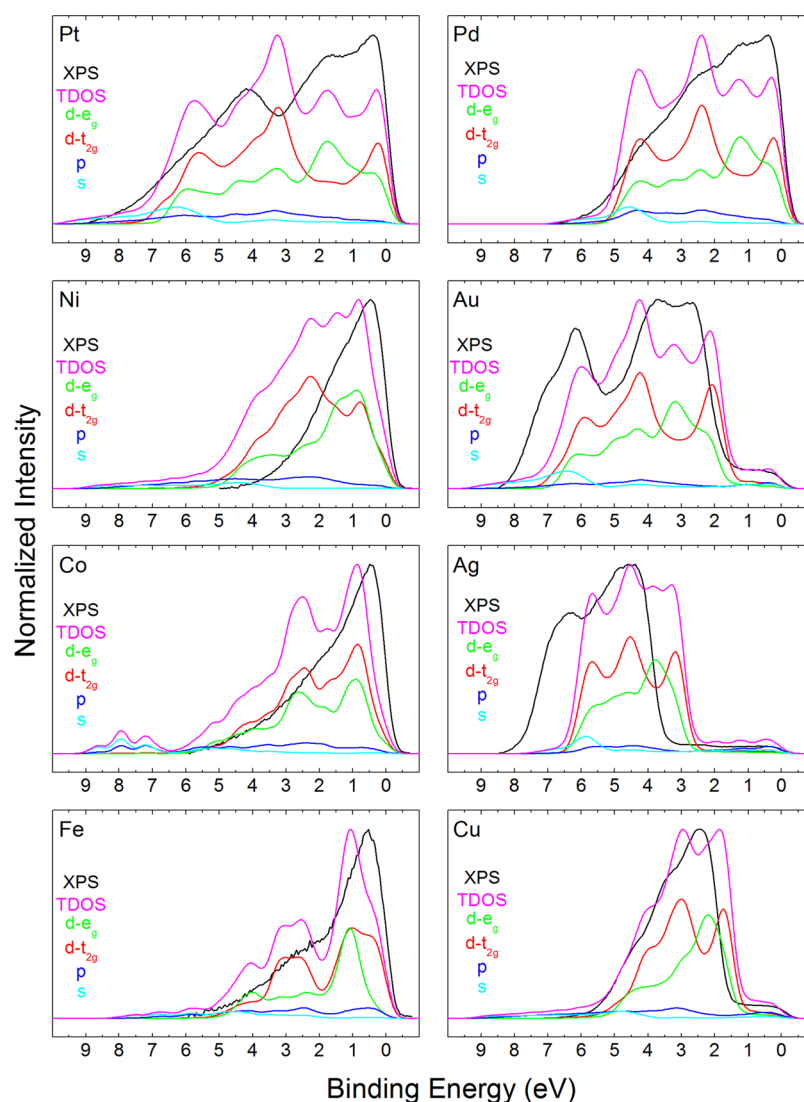


Figure 3. Comparison of experimental XPS valence band spectra after subtraction of a Shirley background (solid black lines) with theoretical DOS (TDOS and symmetry components) of the investigated metal samples, as calculated.

shells (Cu, Ag, Au) vary noticeably less than, in particular, the ones of Fe and Co.

For bulk metals, only experimental d-band centers for Pt and Au have been published to our knowledge.⁸² The measurements of Pt were obtained using photon energies of 90 eV^{27,29,79} and 1486.6 eV,⁸⁰ respectively. Two of the four values obtained with 90 eV (2.356 eV⁷⁹ and 2.54 eV²⁷) are comparable to our UPS-derived results, while the other two reported values for 90 eV excitation (3.45 eV⁸¹ and 3.98 eV²⁹) significantly exceed this range. We note that, due to the low photon energy employed, all of these experiments face the same experimental challenges described above. Lastly, the value of 4.77 eV for Pt determined by Hwang et al.⁸⁰ using monochromatized Al $K\alpha$ radiation is significantly larger than those reported with 90 eV excitation, and also larger than our value of 2.94 (+0.05/-0.10) eV (unfortunately, neither the spectrum, nor the integration limits or background subtraction information is given, and thus the reason for the large deviation is unknown).

For Au, the value of 4.27 eV²⁹ measured with 60 eV photon energy was obtained after subtraction of a Shirley background and using the inflection points of the d-band boundaries as

integration limits. On the basis of the comparable data analysis method of the authors we find their values to agree well with ours [4.32 (+0.10/-0.15) eV for He I and 4.30 (+0.05/-0.05) eV for He II excitation]. Our XPS-based value of 4.45(+0.05/-0.05) eV is slightly higher due to the (improved) determination approach at higher excitation energies.

In summary, thus, we find that experimentally determined d-band centroids are most often determined using photon energies in the UPS regime^{27,29,79,81,83,84} and frequently information on the exact treatment of the background and the selection of integration limits is lacking. In contrast, for the reasons discussed earlier, we favor XPS-based measurements to overcome the challenges associated with low-excitation-energy spectra. Poor correlation of published results using the same photon energy further suggests that a uniform data analysis method is needed for proper comparison.

Comparing our results with previously published DFT-derived d-band center positions, we find rather large deviations, presumably due to the well-known shortcomings of DFT to accurately describe the energies of (localized) d-band states.⁸⁵ An in-depth discussion of differences in the computational models will be published elsewhere.⁸⁶ We focus here on

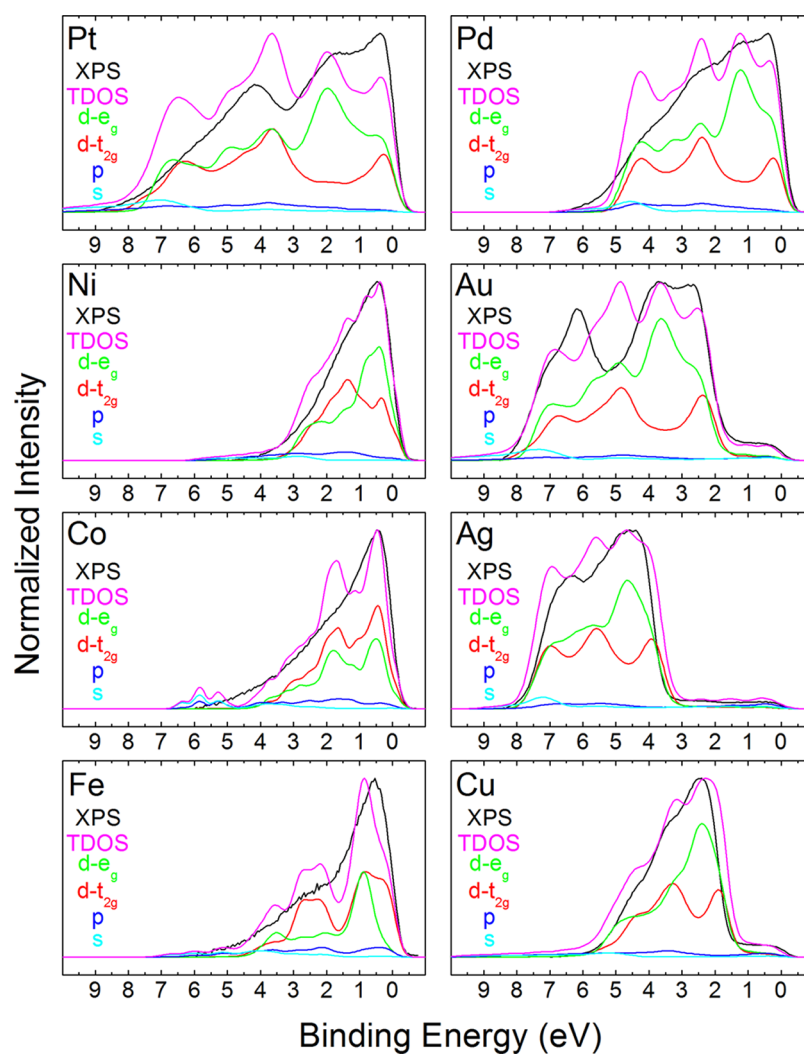


Figure 4. Comparison of experimental XPS valence band spectra (solid black lines) with theoretical DOS (TDOS and symmetry components) of all investigated metal samples after refinement of the calculations.

comparing the theoretical values reported in the literature. The former typically refer to the d-“band” center position of the first atomic layer (the same is true for synchrotron-based photoemission studies with kinetic energies near the minimum of the IMFP curve⁵²). UPS (even lower kinetic energies) and especially XPS (high kinetic energy) measurements average the VBS over a larger volume. Thus, we expect our PES-derived centroid values to be closer to the d-band center calculated for the bulk of the metals (“TDOS”), listed in Table 2. The latter exclude influences of the surface, such as surface defects and the narrowing of surface d-bands, which is considered to be a rather small effect.^{57,87} We find the TDOS centroid (i.e., the d-band center) of Fe, Co, Ni, Pd, and Pt to be higher, the one of Cu to be similar, and the ones of Ag and Au to be lower when compared to the experimentally derived values. The deviations are mainly due to variations in the relative intensity of bands with different symmetries, and in the energy scale between the TDOS and XPS. This can be easily seen in Figure 3, which presents the calculated TDOS along with the symmetry-resolved contributions of the s, p, d- e_g , and d- t_{2g} partial DOS of all metals, and compared to the respective measured XPS VB. When comparing the relative intensities between theory and experiment of the metals in Figure 3, it is noticeable that the VBS at higher binding energies has higher relative intensity in

the calculations than in the XPS experiment. This finding has been reported for numerous transition metals and has been linked to variations of the photoionization cross-section across the d-band.^{88–92} Moreover, Nemoshkalenko et al. found that electrons with e_g symmetry have higher transition probability than those with t_{2g} symmetry.⁹² This explains the larger TDOS d-band center positions of Fe, Co, Ni, Pd, and Pt and shows that theoretical calculations are necessary to obtain the correct intensity distribution in the VBS. For Ag and Au, the energy axis of the TDOS appears to be compressed when compared to the XPS VB. This is not surprising, as DFT is commonly known to underestimate and in some cases also to overestimate the band widths (and band gaps).^{93–101} Therefore, experiments are needed to be able to obtain the correct energy axis. Finally, in the case of Cu, the centroid values of XPS and TDOS are almost identical mathematically, while the visual correlation is quite poor.

Aside from the above-mentioned influences, we expect the omission of surface effects in the TDOS calculations to lead to a slight upward shift of the d-band center, as it is typically narrower at the surface due to the reduced coordination number. This in part explains why the TDOS d-band center values are higher than published DFT results, which take surface effects into account. However, as mentioned earlier, this

effect is rather small, as a comparison of surface d-band centers and bulk d-band centers shows.⁸⁶

3.3. Comparison of the Experimental Spectra with Theoretical DOS, Refinement of the Theoretical Energy Scale. To approximate the true d-band center of the ground state, we have used the experimental energy axis to correct the energy axis of the theoretical DOS. For this purpose, we have refined the calculated DOS by variation of the e_g to t_{2g} ratio in order to achieve the best visual agreement between experiment (after subtraction of a Shirley background) and theory (see Figure 4; this procedure allows for variation in photoionization cross-section between the two symmetries). Furthermore, the energy axis of the DOS spectra was stretched or compressed to visually reconcile the position of prominent features on the binding energy axis. This is a commonly used approach to correct the above-mentioned shortcomings of DFT to determine correct band widths and gaps.^{93–101} For Fe, Co, and Ni, we noticed a shift of the theoretical Fermi position as compared to the experimentally observed position. In these three cases an offset correction was performed. In order to rule out instrumental calibration errors, we have, in addition to our standard three point calibration of the XPS energy scale, verified the Fermi position of the Fe, Co, and Ni XPS VB by referencing the binding energy scale to the position of the Au $4f_{7/2}$ peak at 83.96 eV.³³ No deviation between the two calibration methods was found (within the error of the measurement). We therefore believe that the deviation is due to an upward shift of the theoretical DOS, as previously reported in the case of Fe.¹⁰² The various parameters used to adjust the theoretical DOS are outlined in Table S1 of the Supporting Information.

Overall, the refined theoretical DOS of all metals (Figure 4) fits reasonably well with the experimental spectra (note that this approach still does not include matrix elements and their associated variation of the absolute spectral intensities). The d-band center positions determined in the above-described manner are presented in Table 2 and will be discussed in the following section.

3.4. Comparison of d-Band Center Position with Catalytic Activity. Figure 5a presents a summary of all d-band center positions determined in this work. The bottom half displays the experimentally determined centers, together with the error bars listed in Table 2, while the top half shows the refined calculated d-band center positions of states with e_g and t_{2g} symmetry, as well as their sum (“d-sum”). As mentioned above, we find that the positions determined with He I and He II excitation deviate less than 0.15 eV from each other for all metals (except for Pt, which deviates by 0.7 eV) and are consistently lower than the ones derived by XPS. For reasons discussed earlier, we focus on the comparison between XPS and theory. For the theory portion we only consider the sum of the d-states of e_g and t_{2g} symmetry (“d-sum”) to derive a “true” d-band center energy, while the experimental d-band center also includes contributions from s- and p-states. The influence of the latter is generally rather small: in the case of Cu 3d/Cu 4s and Pt 5d/Pt 6s, the cross section ratios are approximately 44:1 and 75:1, respectively.¹⁰³ When comparing the XPS d-band center positions with the values determined for the refined DOS, it is apparent that the XPS d-band center positions of all metals, except for Fe, are most closely related to their respective e_g center. This supports the work by Nemoshkalenko et al., who found higher photoemission transition probabilities for electrons with e_g symmetry than for those with t_{2g} symmetry.⁹²

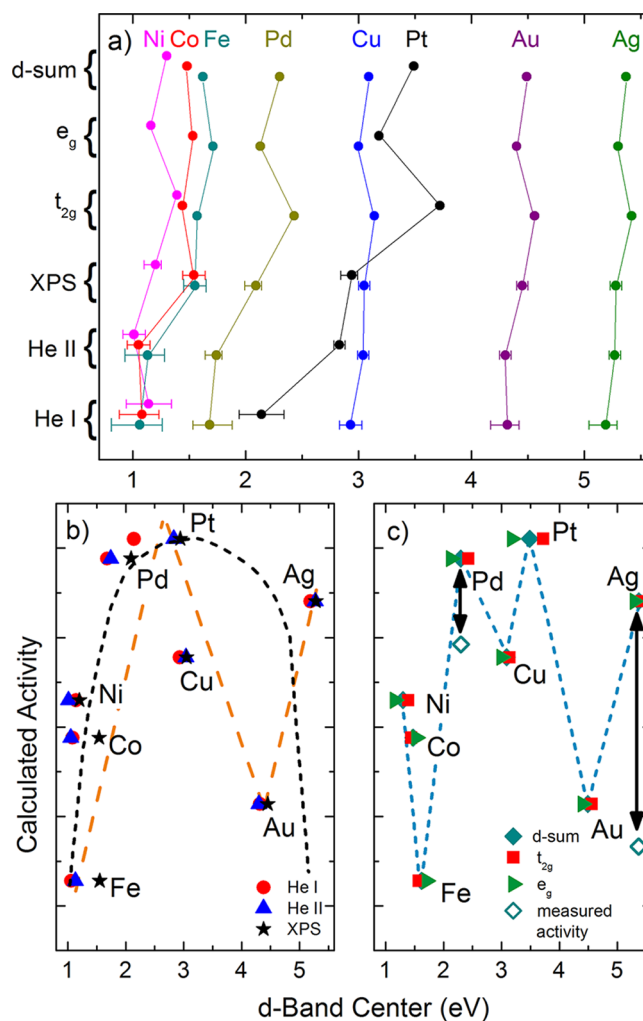


Figure 5. (a) Summary of all derived d-band center positions: experimental (bottom three rows, as a function of excitation energy), and calculated (top three rows, refined and symmetry-selected). (b, c) Calculated activity (taken from ref 26) versus (b) experimental and (c) refined theoretical d-band centers. Black and orange dashed lines in b) are intended as a guide to the eye. The blue dashed line in c) connects the d-sum data points.

Consequently, the XPS d-band center results have to be regarded as a weighted sum of the two symmetry contributions, with a stronger weight given to the e_g component.

Regarding the calculated (and refined) results, we observe that the centroid values for t_{2g} symmetry are higher than for e_g symmetry for all metals with face-centered cubic (fcc) crystal structure (Ni, Cu, Pd, Ag, Pt, Au), and lower only for Fe and Co, which form a body-centered cubic (bcc) and hexagonal close-packed (hcp) lattice, respectively.

It is important to note that the experimentally determined d-band center position of Pt is lower than that of Cu, while the theoretical results predict the reverse order. Furthermore, the experimental Pt center values vary significantly as a function of excitation energy and are lower in value than the theoretical ones. Since Pt is the most active metal for the ORR and its d-band center is often used as a reference or target value, an accurate determination of the Pt d-band center is crucial, and the large deviation between experiment and theory is therefore particularly noteworthy (if not outright worrisome).

Overall, we identify the d-band center values for the refined DOS sum as the best approximation for the true ground-state d-band center, as it combines both the experimental energy axis and the theoretical ground state prediction. In the final section, we will now use these values for comparison with calculated and experimental catalytic activities to provide an experiment-based analysis of the validity of the “d-band center model”. As mentioned, commonly, the dependence of the activity on various parameters like the d-band center,⁷⁸ oxygen binding energy,^{26,104} d-orbital vacancies,¹⁰⁴ etc., yields volcano-shaped curves (so-called “volcano plots”). The various catalytic models are not without controversy, as pointed out by several authors (e.g., Lu et al.,³⁰ Hyman et al.,¹⁰⁵ and Barteau et al.¹⁰⁶). However, none of these studies critically assess the influence of variations in the d-band center. Here, we strive to examine the impact of the refined d-band centers on the commonly used volcano curve dependency rather than to give a detailed discussion of volcano plots and their relevance to catalysis.

Hence, we plotted the experimental and theoretical d-band center positions in Figure 5 panels b and c, respectively, against the calculated ORR activity (taken from Nørskov et al.²⁶). In the following we focus on addressing the correlation of activity with the d-band band center based on a comparison of our experimental and refined theoretical results with published data. In our case, the dashed curve of a somewhat “flattish” volcano (at first sight) appears to give a good description (black, short-dashed line in Figure 5b). However, closer inspection reveals that the trend of the XPS-derived data (black stars in Figure 5b) for Ni, Co, and Fe is not well described, and likewise, that Au and Ag show an inverted trend. Furthermore, the Cu value is a complete outlier. In fact, an “N”-shaped (zigzag) curve gives a better description (orange, long-dashed line in Figure 5b), with a (volcano-type) maximum at lower d-band center values and an additional increase in activity at the higher d-band center value of Ag. Furthermore, by simply connecting the d-sum data points in order of their d-band center position (blue, short-dashed line in Figure 5c), a complex (apparently random) dependency emerges. The Pt–Cu discrepancy is not surprising—both exhibit similar d-band center values, but the overall d-band structure (including the overall width and the density of states near the Fermi energy) is vastly different (see Figure 2).

To take into account possible differences on the activity scale between theory and experiment, we have also included experimental activities measured in alkaline electrolyte by Lima et al. on single crystal metals (Pd, Pt, Au, and Ag)⁷⁸ in Figure 5c. To align the ordinate scales of the works by Nørskov et al.²⁶ and Lima et al.,⁷⁸ we have aligned the Pt and Au data points (for d-sum), assuming a linear relationship between the theoretically determined and electrochemically observed activities. Thus, only two experimental electrochemical data points are visible in Figure 5c (for Pd and Ag), while the Pt and Au data points coincide with the “d-sum” data points (per construction). With this additional modification, we find that both the Pd and the Ag experimental activities are lower than theoretically predicted (compared to the Pt and Au reference activities indicated by double-headed arrows in Figure 5c), and that modifications to the original volcano shape introduced by our d-band centers persist.

Furthermore, as suggested by Hyman et al.¹⁰⁵ in a theoretical study, one would expect the DOS near the Fermi energy to influence the adsorption energy of the O species. They noted that, in cases where there was a lack of correlation between

shifts of the d-band center energy and the binding energy of O species, the cause was a lack of correlation between the d-band centers and the DOS near the Fermi energy. Indeed, based on a reduction of intensity at the Fermi energy, previous studies (e.g., refs 46 and 107) suggest that t_{2g} states located near the Fermi energy are important for adsorption. This is corroborated by our findings for almost all metals studied herein: the t_{2g} states clearly dominate this region of the DOS (see Figure 3).

To gain improved insight into the correlation of the electronic structure and activity, experimental and theoretical efforts should be combined to extract catalytically active states. To summarize this discussion, we thus reason that there is no simple direct relationship between the energy of the d-band center and the ORR catalytic activity of transition metals. In particular the proximity of the d-band center positions of Fe, Co, and Ni, as well as of Pt and Cu (despite the large differences in activity of these metals) suggests that the position of the d-band center alone is not a representative measure to evaluate the ORR activity.

4. CONCLUSIONS

To test the validity of models relating the catalytic activity and the single parameter “d-band center position”, we have investigated the valence band structure of various noble and transition metals by photoelectron spectroscopy (PES) using He I, He II, and monochromatized Al $K\alpha$ excitation. Our results show that final states effects, the photoionization cross-section, and adsorption of residual gas molecules in an ultrahigh vacuum environment strongly influence the valence band structure. We find that valence bands recorded with monochromatized Al $K\alpha$ radiation are most closely comparable to the ground state density of states. We demonstrate that the XPS-derived energy scale can be used to correct the DOS calculations in order to draw conclusions about the true ground-state d-band structure. Our data show that the dependence of ORR activity on d-band center position is more complex than a simple continuous (volcano-plot) distribution.

■ ASSOCIATED CONTENT

📄 Supporting Information

Refinement parameters applied to the calculated DOS and UPS He I valence band spectra of a polycrystalline Pd foil immediately after Ar^+ sputtering and after one day of storage in UHV. This material is available free of charge via the Internet at <http://pubs.acs.org>.

■ AUTHOR INFORMATION

Corresponding Author

*E-mail: hofmann@unlv.nevada.edu; heske@unlv.nevada.edu.

Notes

The authors declare no competing financial interest.

■ ACKNOWLEDGMENTS

We gratefully acknowledge funding by the U.S. Department of Energy, Prime Contract No. DE-AC02-06CH11357 (ANL) and ANL Subcontract Nos. 7F-01041 (UNLV) and 7F-01321 (Caltech). M.B. acknowledges support by the Impuls- und Vernetzungsfonds of the Helmholtz-Association (VH-NG-423).

REFERENCES

- (1) Ertl, G. *Angew. Chem., Int. Ed.* **2008**, *47*, 3524–3535.
- (2) Bowker, M. *The Basis and Applications of Heterogeneous Catalysis*; Oxford University Press: New York, U.S.A., 1998.
- (3) Rothenberg, G. *Catalysis: Concepts and Green Applications*; Wiley-VCH: Weinheim, Germany, 2008.
- (4) Baer, Y.; Hedén, P. F.; Hedman, J.; Klasson, M.; Nordling, C.; Siegbahn, K. *Phys. Scr.* **1970**, *1*, 55–65.
- (5) Battye, F. L.; Goldmann, A.; Kasper, L.; Hüfner, S. *Z. Phys. B* **1977**, *27*, 209–214.
- (6) Hüfner, S.; Wertheim, G. K. *Phys. Lett. A* **1974**, *47*, 349–350.
- (7) Borup, R.; Meyers, J.; Pivovar, B.; Kim, Y. S.; Mukundan, R.; Garland, N.; Myers, D.; Wilson, M.; Garzon, F.; Wood, D.; et al. *Chem. Rev.* **2007**, *107*, 3904–3951.
- (8) Popov, B. N.; Li, X.; Liu, G.; Lee, J.-W. *Int. J. Hydrogen Energy* **2011**, *36*, 1794–1802.
- (9) Carlson, E.; Kopf, P.; Sinha, J.; Sriramulu, S.; Yang, Y. *PEM Fuel Cell Cost Status, Fuel Cell Seminar*, Palm Springs, CA, 2005, Abstract No. 392.
- (10) Costamagna, P.; Srinivasan, S. *J. Power Sources* **2001**, *102*, 242–252.
- (11) Gewirth, A. A.; Thorum, M. S. *Inorg. Chem.* **2011**, *49*, 3557–3566.
- (12) Morozan, A.; Jusselme, B.; Palacin, S. *Energy Environ. Sci.* **2011**, *4*, 1238–1254.
- (13) Chen, Z.; Higgins, D.; Yu, A.; Zhang, L.; Zhang, J. *Energy Environ. Sci.* **2011**, *4*, 3167–3192.
- (14) Guo, S.; Wang, E. *Nano Today* **2011**, *6*, 240–264.
- (15) Wang, X.; Kariuki, N.; Niyogi, S.; Smith, M. C.; Myers, D. J.; Hofmann, T.; Zhang, Y.; Bär, M.; Heske, C. *ECS Trans.* **2008**, 109–119.
- (16) Wang, X.; Kariuki, N.; Vaughey, J. T.; Goodpaster, J.; Kumar, R.; Myers, D. J. *J. Electrochem. Soc.* **2008**, *155*, B602–B609.
- (17) Bing, Y.; Liu, H.; Zhang, L.; Ghosh, D.; Zhang, J. *Chem. Soc. Rev.* **2010**, *39*, 2184.
- (18) Hammer, B.; Nørskov, J. K. *Surf. Sci.* **1995**, *343*, 211–220.
- (19) Shao, M.; Liu, P.; Zhang, J.; Adzic, R. J. *Phys. Chem. B* **2007**, *111*, 6772–6775.
- (20) Ruban, A.; Hammer, B.; Stoltze, P.; Skriver, H.; Nørskov, J. *J. Mol. Catal. A-Chem.* **1997**, *115*, 421–429.
- (21) Greeley, J.; Nørskov, J. K. *Surf. Sci.* **2005**, *592*, 104–111.
- (22) Hammer, B.; Nørskov, J. K. *Adv. Catal.* **2000**, *45*, 71–129.
- (23) Stamenkovic, V.; Mun, B. S.; Mayrhofer, K. J. J.; Ross, P. N.; Markovic, N. M.; Rossmeisl, J.; Greeley, J.; Nørskov, J. K. *Angew. Chem., Int. Ed.* **2006**, *45*, 2897–2901.
- (24) Kitchin, J. R.; Nørskov, J. K.; Barteau, M. A.; Chen, J. G. *J. Chem. Phys.* **2004**, *120*, 10240–10246.
- (25) Hyman, M. P.; Loveless, B. T.; Medlin, J. W. *Surf. Sci.* **2007**, *601*, 5382–5393.
- (26) Nørskov, J. K.; Rossmeisl, J.; Logadottir, A.; Lindqvist, L.; Kitchin, J. R.; Bligaard, T.; Jónsson, H. *J. Phys. Chem. B* **2004**, *108*, 17886–17892.
- (27) Mun, B. S.; Watanabe, M.; Rossi, M.; Stamenkovic, V.; Markovic, N. M.; Ross, P. N. *J. Chem. Phys.* **2005**, *123*, 204717.
- (28) Kibler, L. A.; El-Aziz, A. M.; Hoyer, R.; Kolb, D. M. *Angew. Chem., Int. Ed.* **2005**, *44*, 2080–2084.
- (29) Toyoda, E.; Jinnouchi, R.; Hatanaka, T.; Morimoto, Y.; Mitsuhashi, K.; Visikovskiy, A.; Kido, Y. *J. Phys. Chem. C* **2011**, *115*, 21236–21240.
- (30) Lu, C.; Lee, I. C.; Masel, R. I.; Wieckowski, A.; Rice, C. J. *Phys. Chem. A* **2002**, *106*, 3084–3091.
- (31) Xin, H.; Limic, S. *J. Chem. Phys.* **2010**, *132*, 221101.
- (32) Gajdo, M.; Eichler, A.; Hafner, J. *J. Phys.: Condens. Matter* **2004**, *16*, 1141–1164.
- (33) Seah, M. P. *Surf. Interface Anal.* **2001**, *31*, 721–723.
- (34) Schultz, P. *SeqQuest, Electronic Structure Code*; Sandia National Laboratory, Albuquerque, NM: <http://dft.sandia.gov/Quest/>.
- (35) Edwards, A. *SeqQuest, Post Analysis Code*; Sandia National Laboratory, Albuquerque, NM: http://dft.sandia.gov/Quest/SeqQ_Kudos.
- (36) Perdew, J. P.; Burke, K.; Ernzerhof, M. *Phys. Rev. Lett.* **1996**, *77*, 3865–3868.
- (37) Ceperley, D. M.; Alder, B. J. *Phys. Rev. Lett.* **1980**, *45*, 566–569.
- (38) Perdew, J. P.; Zunger, A. *Phys. Rev. B* **1981**, *23*, 5048–5079.
- (39) Goddard, W. A. *Phys. Rev.* **1968**, *174*, 659–662.
- (40) Melius, C. F.; Goddard, W. A. *Phys. Rev. A* **1974**, *10*, 1528–1540.
- (41) Moulder, J. F.; Stickle, W. F.; Sobol, P. E. *Handbook of X-Ray Photoelectron Spectroscopy*; Perkin-Elmer, Physical Electronics Division: Eden Prairie, U.S.A., 1993.
- (42) Küppers, J.; Conrad, H.; Ertl, G.; Latta, E. E. *Jpn. J. Appl. Phys.* **1974**, *2*, 225–228.
- (43) Tran, I. C.; Félix, R.; Bär, M.; Weinhardt, L.; Zhang, Y.; Heske, C. *J. Am. Chem. Soc.* **2010**, *132*, 5789–5792.
- (44) Paál, Z.; Schlögl, R.; Ertl, G. *Faraday Trans.* **1992**, *88*, 1179–1189.
- (45) Conrad, H.; Ertl, G.; Koch, J.; Latta, E. E. *Surf. Sci.* **1974**, *43*, 462–480.
- (46) Shirley, D. A.; Stöhr, J.; Wehner, P. S.; Williams, R. S.; Apai, G. *Phys. Scr.* **1977**, *16*, 398–413.
- (47) Stöhr, J.; McFeely, F. R.; Apai, G.; Wehner, P. S.; Shirley, D. A. *Phys. Rev. B* **1976**, *14*, 4431–4438.
- (48) Feibelman, P. J.; Eastman, D. E. *Phys. Rev. B* **1974**, *10*, 4932–4947.
- (49) Hüfner, S. *Photoelectron Spectroscopy: Principles and Applications*; Springer: Heidelberg, Germany, 2003.
- (50) Markovic, N. M.; Gasteiger, H. A.; Ross, P. N. *J. Phys. Chem.* **1995**, *99*, 3411–3415.
- (51) Wehner, P. S.; Stöhr, J.; Apai, G.; McFeely, F. R.; Williams, R. S.; Shirley, D. A. *Phys. Rev. B* **1976**, *14*, 2411–2416.
- (52) Seah, M. P.; Dench, W. A. *Surf. Interface Anal.* **1979**, *1*, 2–11.
- (53) Powell, C. J. *Surf. Sci.* **1974**, *44*, 29–46.
- (54) Powell, C. J.; Jablonski, A. *J. Phys. Chem. Ref. Data* **1999**, *28*, 19–62.
- (55) Tanuma, S.; Powell, C. J.; Penn, D. R. *Surf. Interface Anal.* **1993**, *20*, 77–89.
- (56) Oura, K. *Surface Science: An Introduction*; Springer: New York, 2003.
- (57) Zangwill, A. *Physics at Surfaces*; Cambridge University Press: Cambridge, UK, 1988.
- (58) Davison, S. G.; Stęślicka, M. *Basic Theory of Surface States*; Clarendon Press: Oxford, UK, 1996.
- (59) Lloyd, D. R.; Quinn, C. M.; Richardson, N. V. In *Surface and Defect Properties of Solids*; Roberts, M. W., Thomas, J. M., Eds.; The Royal Society of Chemistry: London, UK, 1977; Vol. 6, pp 179–217.
- (60) Haydock, R.; Kelly, M. J. *Surf. Sci.* **1973**, *38*, 139–148.
- (61) Steiner, P.; Hüfner, S.; Freeman, A. J.; Wang, D. *Solid State Commun.* **1982**, *44*, 619–622.
- (62) Brundle, C. R. *Surf. Sci.* **1977**, *66*, 581–595.
- (63) Yu, K. Y.; Spicer, W. E.; Lindau, I.; Pianetta, P.; Lin, S. F. *Surf. Sci.* **1976**, *57*, 157–183.
- (64) Frerichs, M.; Schweiger, F. X.; Voigts, F.; Rudenkiy, S.; Maus-Friedrichs, W.; Kempter, V. *Surf. Interface Anal.* **2005**, *37*, 633–640.
- (65) Castro, G.; Hülse, J. E.; Küppers, J.; Gonzalez-Eliphe, A. R. *Surf. Sci.* **1982**, *117*, 621–628.
- (66) Joyner, R. W.; Roberts, M. W. *J. Chem. Soc., Faraday Trans. 1* **1974**, *70*, 1819–1824.
- (67) Page, P. J.; Trimm, D. L.; Williams, P. M. *J. Chem. Soc., Faraday Trans. 1* **1974**, *70*, 1769–1781.
- (68) Norton, P.; Tapping, R.; Goodale, J. *Surf. Sci.* **1978**, *72*, 33–44.
- (69) Conrad, H.; Ertl, G.; Küppers, J.; Latta, E. E. *Solid State Commun.* **1975**, *17*, 613–616.
- (70) Gustafsson, T.; Plummer, E. W.; Eastman, D. E.; Freeouf, J. L. *Solid State Commun.* **1975**, *17*, 391–396.

- (71) L egar e, P.; Hilaire, L.; Maire, G.; Krill, G.; Amamou, A. *Surf. Sci.* **1981**, *107*, 533–546.
- (72) Conrad, H.; Ertl, G.; K uppers, J.; Latta, E. E. *Faraday Discuss. Chem. Soc.* **1974**, *58*, 116–124.
- (73) Boronin, A. I.; Koscheev, S. V.; Zhidomirov, G. M. *J. Electr. Spectrosc. Rel. Phenom.* **1998**, *96*, 43–51.
- (74) Kiskinova, M.; Pirug, G.; Bonzel, H. P. *Surf. Sci.* **1983**, *133*, 321–343.
- (75) Atkinson, S. J.; Brundle, C. R.; Roberts, M. W. *Faraday Discuss. Chem. Soc.* **1974**, *58*, 62–79.
- (76) Stamenkovic, V. R.; Fowler, B.; Mun, B. S.; Wang, G.; Ross, P. N.; Lucas, C. A.; Markovi c, N. M. *Science* **2007**, *315*, 493–497.
- (77) Shao, M. H.; Huang, T.; Liu, P.; Zhang, J.; Sasaki, K.; Vukmirovic, M. B.; Adzic, R. R. *Langmuir* **2006**, *22*, 10409–10415.
- (78) Lima, F. H. B.; Zhang, J.; Shao, M. H.; Sasaki, K.; Vukmirovic, M. B.; Ticianelli, E. A.; Adzic, R. R. *J. Phys. Chem. C* **2007**, *111*, 404–410.
- (79) Ross, P. N.; Markovi c, N. M. *DOE Annual Hydrogen Review*; Department of Energy: Washington, DC, 2004.
- (80) Hwang, S. J.; Yoo, S. J.; Jang, S.; Lim, T.-H.; Hong, S. A.; Kim, S.-K. *J. Phys. Chem. C* **2011**, *115*, 2483–2488.
- (81) Toyoda, E.; Hatanaka, T.; Takahashi, N.; Jinnouchi, R.; Morimoto, Y. *ECS Trans.* **2009**, *25*, 1057–1064.
- (82) Web of Science Search for keywords “d-band center” and “photoemission”, September 3, 2012.
- (83) Kim, Y. S.; Mun, B. S.; Ross, P. N. *Curr. Appl. Phys.* **2011**, *11*, 1179–1182.
- (84) Visikovskiy, A.; Matsumoto, H.; Mitsuhara, K.; Nakada, T.; Akita, T.; Kido, Y. *Phys. Rev. B* **2011**, *83*, 165428.
- (85) Ziman, J. M.; Mott, S. N. F.; Hirsch, P. B. *The Physics of Metals*; Cambridge University Press: Cambridge, UK, 1969.
- (86) Yu, T. H.; Hofmann, T.; Sha, Y.; Merinov, B. V.; Heske, C.; Goddard, W. A. *to be published* **2012**.
- (87) Kokalj, A.; Caus a, M. *J. Phys.: Condens. Matter* **1999**, *11*, 7463–7480.
- (88) Smith, N. V.; Wertheim, G. K.; H ufner, S.; Traum, M. M. *Phys. Rev. B* **1974**, *10*, 3197–3206.
- (89) Nemoshkalenko, V. V.; Aleshin, V. G.; Kucherenko, Y. N.; Sheludchenko, L. M. *Solid State Commun.* **1974**, *15*, 1745–1747.
- (90) Shevchik, N. J. *Phys. Rev. B* **1976**, *13*, 4217–4220.
- (91) H ochst, H.; H ufner, S.; Goldmann, A. *Phys. Lett. A* **1976**, *57*, 265–266.
- (92) Nemoshkalenko, V. V.; Aleshin, V. G.; Kucherenko, Y. N.; Sheludchenko, L. M. *J. Electr. Spectrosc. Rel. Phenom.* **1975**, *6*, 145–150.
- (93) Weinhardt, L.; Fuchs, O.; Umbach, E.; Heske, C.; Fleszar, A.; Hanke, W.; Denlinger, J. D. *Phys. Rev. B* **2007**, *75*, 165207.
- (94) Heske, C.; Treusch, R.; Himpfel, F. J.; Kakar, S.; Terminello, L. J.; Weyer, H. J.; Shirley, E. L. *Phys. Rev. B* **1999**, *59*, 4680–4684.
- (95) Sashin, V. A.; Dorsett, H. E.; Bolorizadeh, M. A.; Ford, M. J. *J. Chem. Phys.* **2000**, *113*, 8175–8182.
- (96) Northrup, J. E.; Hybertsen, M. S.; Louie, S. G. *Phys. Rev. Lett.* **1987**, *59*, 819–822.
- (97) Northrup, J. E.; Hybertsen, M. S.; Louie, S. G. *Phys. Rev. B* **1989**, *39*, 8198–8208.
- (98) Mahan, G. D.; Sernelius, B. E. *Phys. Rev. Lett.* **1989**, *62*, 2718–2720.
- (99) Shirley, E. L. *Phys. Rev. B* **1996**, *54*, 7758–7764.
- (100) Jensen, E.; Plummer, E. W. *Phys. Rev. Lett.* **1985**, *55*, 1912–1915.
- (101) Lyo, I.-W.; Plummer, E. W. *Phys. Rev. Lett.* **1988**, *60*, 1558–1561.
- (102) H ochst, H.; Goldmann, A.; H ufner, S. *Z. Phys. B* **1976**, *24*, 245–250.
- (103) Yeh, J. J.; Lindau, I. *Atomic Data Nucl. Data Tables* **1985**, *32*, 1–155.
- (104) Appleby, A. J. *Catal. Rev.* **1971**, *4*, 221–224.
- (105) Hyman, M. P.; Medlin, J. W. *J. Phys. Chem. C* **2007**, *111*, 17052–17060.
- (106) Barteau, M. A. *Catal. Lett.* **1991**, *8*, 175–183.
- (107) Clarke, T. A.; Gay, I. D.; Mason, R. *Chem. Phys. Lett.* **1974**, *27*, 172–174.
- (108) Hall, G. K.; Mee, C. H. B. *Phys. Stat. Sol. (a)* **1971**, *5*, 389–395.
- (109) Anderson, P. A. *Phys. Rev.* **1949**, *76*, 388–390.
- (110) White, K. *Physical Properties of the Platinum Metals. Platinum Met. Rev.* **1972**, *59*.